KING'S College LONDON

University of London

Concentric Tube Robot – A Modular Design for Achieving Two Controllable Sections and a Stereo Tracking System.

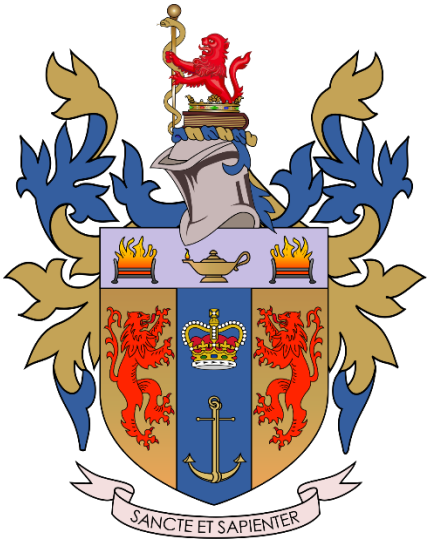

The Hung Dang

Supervisors:
Dr Carlo A. Seneci
Professor Christos Bergeles

Submitted in partial fulfilment of
the Master of Science in Healthcare Technologies

August 2024

Table of Contents

PROJECT PLAN

I. Background

Optic nerve sheath fenestration (ONSF) is a surgical procedure that involves incising the optic nerve sheath to decompress and protect the optic nerve in patients with elevated intracranial pressure [1]. Concentric tube robots (CTR) are continuum robots made by nesting tubes of different sizes [2]. Their slenderness and flexibility make them promising candidates for minimally invasive surgery, especially in eye operations [3]. By translating and rotating tubes of different curvatures, one can change the curvature of the combined tubes, allowing for steering of the CTR's tips and navigation through complex spaces.

However, controlling CTR remains a challenge, as the tubes can be considered to have an infinite degree of freedom. A balanced pair of tubes refers to a concept where a combined tube can be made to curve into a straight one by rotating two individual tubes [2]. Slots on nitinol tubes help reduce the bending stiffness, which aids in the process of creating a balanced pair. Researchers at King's College London have succeeded in developing a balanced pair of nitinol tubes for CTR by laser-machining slots on the larger tube, enabling control of one curved section. For validation, various methods exist for tracking the tips of the CTR; however, controlling the CTR entails changing the entire tube configuration [4], [5], leading to the requirement for a system that can follow the movement of the whole CTR.

II. Aims

The primary aim of this project is to develop a design that adds a second curved section that can be controlled independently from the first section of the CTR with four nitinol tubes. Additionally, this project seeks to build and develop an algorithm for 3D tracking of the entire CTR.

III. Deliverables

1. Design how the nitinol tubes should be placed, and which sections should be laser-machined.
2. Perform finite element analysis to find the best patterns on tube 2 and tube 4 to create two balanced pairs for the CTR system and send them to another party for manufacturing.
3. Purchase cameras for the stereo tracking system, design a mechanism to fix them, and write a script for calibrating the cameras to obtain the relative coordinates of the cameras in world frame.
4. Write a script to perform segmentation and 3D reconstruction of the entire CTR from two cameras
5. Design and purchase necessary components to assemble the actuation system for controlling the tubes.
6. Receive the machined nitinol tubes from the third party, assemble the whole system and perform validation.

IV. Workplan & Timelines

Deliverables	Week 1-2 (03/06-16/06)	Week 3-4 (17/06-30/06)	Week 5-6 (01/07-14/07)	Week 7-8 (15/07-28/07)	Week 9-10 (29/07-04/08)	Week 11-12 (05/08-18/08)
1	x					
2		x				
3			x			
4				x		
5					x	
6						x

STATEMENT ON THE USE OF AI TOOLS

I declare that parts of this submission have contributions from AI software and that it aligns with acceptable use as specified as part of the assignment brief/ guidance and is consistent with good academic practice. The content can still be considered as my own words. I understand that as long as my use falls within the scope of appropriate use as defined in the assessment brief/guidance then this declaration will not have any direct impact on the grades awarded.

I acknowledge use of software to:

(i) Suggest structure and assist with understanding core concepts.

(ii) Rephrase and paraphrase parts of this essay.

(iii) Generate code as examples for developing the algorithms.

ChatGPT [6] and Claude [7] were used for all of the aforementioned purposes.

ACKNOWLEDGEMENTS

This project was conducted under the supervision of Dr. Carlo Alberto Seneci and Professor Christos Bergeles. The 3D printing of the designs was supported by Mr. Jaye Barrington. The nitinol tubes were manufactured by the Manufacture of Active Implants and Surgical Instruments (MAISI).

ABSTRACT

Introduction: Concentric tube robots (CTR) are very slender and flexible, making them suitable for minimally invasive eye surgery. Researchers at King's College London previously manufactured a balanced pair of nitinol tubes for CTR, allowing the combined tubes to be straightened or curved by rotating two individual tubes. No system is currently available for 3D tracking the entire CTR. This project aims to develop a novel design to add a second controllable curved section using four tubes and create a stereo vision system for 3D tracking the entire CTR.

Method: Slot patterns were designed and laser-machined on the 2nd and 4th largest tubes. Finite element analysis was done to select the best patterns, so that the bending stiffness of tube 2 matches that of tube 1 and the bending stiffness of tube 4 matches the combination of other three. An actuation system was CAD-designed to rotate and translate the tube system. Images of the CTR captured by two stereo cameras were segmented and processed to reconstruct its 3D coordinates using epipolar geometry.

Result: The slot patterns on tube 2 and tube 4 successfully reduce the bending stiffness. Rotating tube 2 straightened the combined curve of tubes 1 and 2. Rotating tube 4 straightened the combined curve of all four tubes. In the final assembly, the curvature, rotation, and translation of the second added curve section can be controlled independently from the first section. Additionally, the 3D tracking system successfully reconstructed the CTR with an update rate of 8 Hz.

Conclusion: The project created an original compact design to add a second controllable section to CTR and developed a novel 3D tracking system for the entire robot. Future work could focus on validating the system on 3D model and refining the 3D stereo tracking system.

ABBREVIATIONS

BTSR: bending-to-torsional stiffness ratio

CNC: computer numerical control

CTR: concentric tube robots

DOF: degrees of freedom

FEA: finite element analysis

GMM: gaussian mixture model

ONSF: optic nerve sheath fenestration

1 INTRODUCTION

1.1 Concentric tube robots and their medical applications

Concentric tube robots (CTR) are made by small tubes of different sizes nested together. By using tubes with very small diameters (0-2mm), we can create compact, slender, and flexible robots that can go through narrow and complex pathways. As many rigid surgical tools tend to be bulky and require certain openings to advance to the target, this capability of CTR is advantageous in surgical applications.

The robot in this project is targeted for the optic nerve sheath fenestration (ONSF) procedure. In elevated intracranial pressure, the increased pressure compresses the optic nerve, potentially leading to permanent vision damage if left untreated [1]. During ONSF, surgeons make an incision on the optic nerve sheath to relieve the nerve. However, the optic nerve is located behind the eyeballs, making it hard for the surgeon to access it without making a large incision and significant manipulation of the nerve. CTR, with their advantage in size and shape, could follow the curve of the eyeballs to access the nerve and offer a minimally invasive solution [3].

In controlling CTR, if the overlapping sections of two nested tubes are curved, when one tube rotates with respect to the other, the combined curvature changes. Utilizing this mechanism, scientists have proposed the concept of balanced-stiffness tube pair (hereinafter, balanced pair), where the combined curvature of two tubes reaches its maximum if rotated in the same direction (Figure 1a) and becomes zero if rotated in opposite directions (Figure 1b).

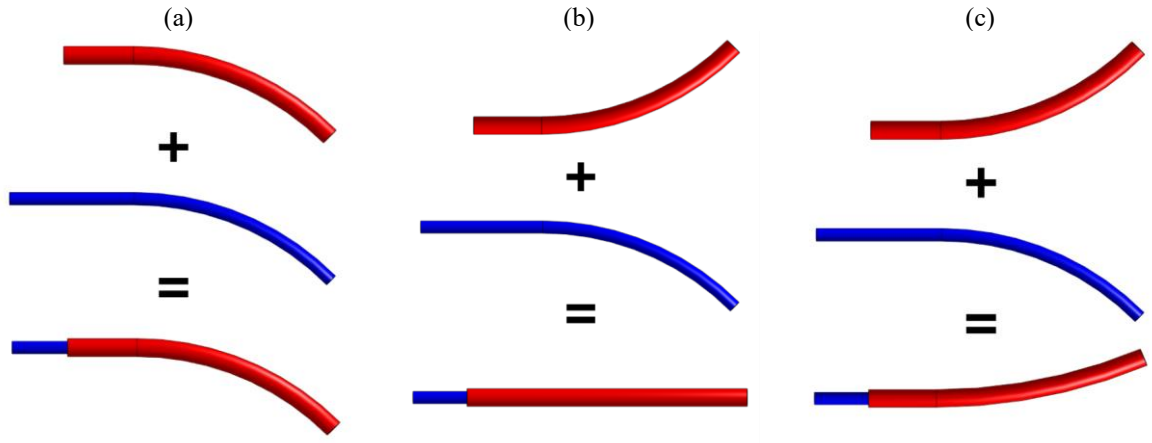

Figure 1. Illustration for the concept of balanced pair. In an ideal balanced pair, the combined tubes will reach maximum curve if 2 tubes are rotated in the same directions (a) and become straight if they are opposite (b). However, in reality, two random tubes could not achieve such results (c).

Balanced pairs offer a method for steering the tube ends by simply rotating the tubes [2]. Nitinol is the most commonly used material for CTR due to its superelasticity, allowing the curvature of the tubes to change significantly without permanent deformation [8]. Additionally, its shape-memory effect enables manufacturers to create tubes with necessary curvature from commercially available ones.

1.2 Current challenges in design, manufacturing, and control

Creating a balanced pair between two nitinol tubes is not straightforward. Since the tubes need to be nested, their diameters and thicknesses differ. If each individual tube has the same curvature, the combined assembly will curve in the direction of the tube with higher stiffness (from now on, “stiffness” will refer to the characteristics of the entire structure rather than the properties of the materials). To address this issue, slots with different sizes and patterns are laser-machined on the tube to reduce the overall stiffness [9], [10]. However, different slot patterns impact the tubes in distinct ways, and finite element analysis (FEA) techniques are needed for predicting the behavior of the laser-machined tubes. Even after conducting FEA, the resulting tubes may not perform as expected.

The instability of CTR, mainly referred to as the snapping phenomenon, poses a significant challenge and is an active research area [11]. This effect is attributed to a high bending-to-torsional stiffness ratio (BTSR). When two tubes are rotated apart at a certain twist angle, the strain energy is released, and the tube tip is forced to rotate to a more stable position. Such sudden movement can cause tissue damage and is risky in a surgical environment.

Controlling the CTR presents additional challenges. Although many research groups have developed sensing systems for tracking the tips to aid in researching CTR’s behavior and control [12], [13], [14], due to their continuum properties, CTR can be considered to have infinite degrees of freedom (DOF), and the overall shape of the entire tube body, not only the distal tips, changes with any individual tube rotation. While the forward kinematics model can be calculated by solving a one-dimensional Cosserat rods problem [3], [15], this approach requires numerical solutions, and might not be practical in real-time applications. This necessitates a method for tracking the entire tube for evaluation and advance control strategy.

One approach to CTR tracking is using electromagnetic tracking systems [16], [17]. Even with its accuracy, its implementation is costly and necessitates a complicated setup [4]. Another alternative is to use stereo cameras, which involve setting up two cameras and comparing their images to recreate the 3D image [5]. Given the availability of commercial cameras, this method provides a cheaper solution. Furthermore, the cameras can extract all information about the CTR rather than just some specific point in the electromagnetic systems.

1.3 Project aim and objectives

Previously, researchers at King’s College London successfully built a CTR using a balanced pair of nitinol tubes. They accomplished this by machining circular slots on the larger tube in an isotropic pattern around the axis. The slot patterns were first designed and simulated on commercial software for computer-aided design (CAD) and FEA, and then cut with a laser cutter. The team achieved a balanced pair where they can control a 2 cm curved section to transit from a curve to a straight configuration (Figure 2) Their project continues by adding a third tube, trying to add another controllable curved section. Additionally, the team has developed a system for tracking the tips of the CTR, further supporting the research into CTR modeling and control [18].

(a)

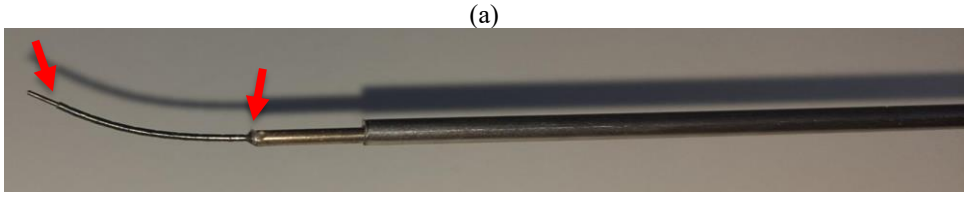

(b)

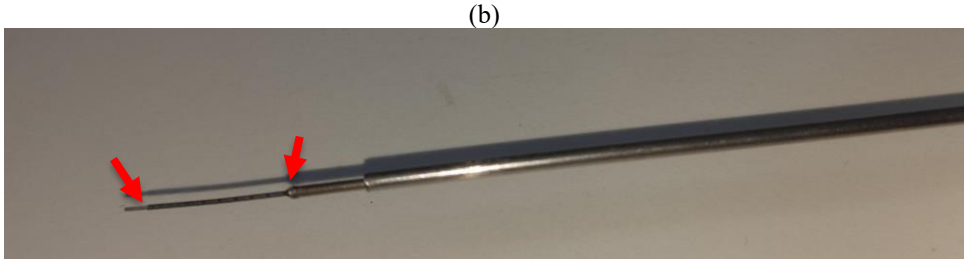

Figure 2. Balanced pair previously created by King's research team when the tubes are rotated in the same (a) and opposite direction (b). The red arrows indicate the start and end of the controllable section.

This project is built on the team's previous work. We aim to achieve a second in dependently controllable balanced pair by adding more tubes to the system as well as to build a stereo tracking system for monitoring the entire CTR, rather than just the tip.

The objectives for achieving the second dependently controllable balanced pair are:

- Design a new arrangement for curve and straight sections in each tube and between tubes to achieve two independently controllable pairs.
- Design slot patterns and perform FEA to identify the best patterns for creating balanced pairs.
- Design an actuation system to achieve 6 DOF for 2 controllable curves.
- Assemble and test the system for stability.

The objectives for developing the stereo camera system are:

- Setting two cameras for tracking the CTR.
- Segmentation of the tubes from two cameras.
- Matching the features from 2 cameras and reconstructing 3D coordinates of the tubes.

2 METHODOLOGY

2.1 Terminology definition and problem simplification

For simplification, in both design and stereo tracking, tubes were considered 1-dimensional (1D) shapes constituted by straight lines and arcs (Figure 3).

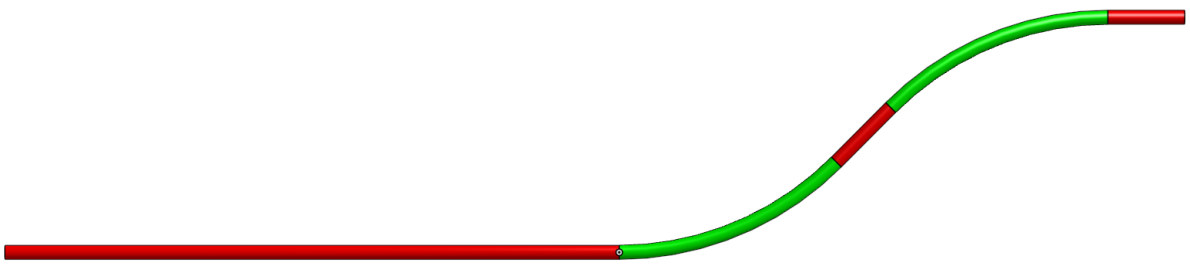

Figure 3. The tubes are simplified into 1D shapes comprising of straight lines (red) and arcs (green).

To create a CTR, multiple tubes are nested within one another. In this thesis, the result tubes after combining two or more tubes are referred to as “combined tubes.” Each individual tube used for creating the combined tubes can have multiple “curved sections” and “straight sections” (green and red sections in Figure 3, respectively). Each individual nitinol tube has two DOF that we can control: rotation (twisting) and translation (Figure 4).

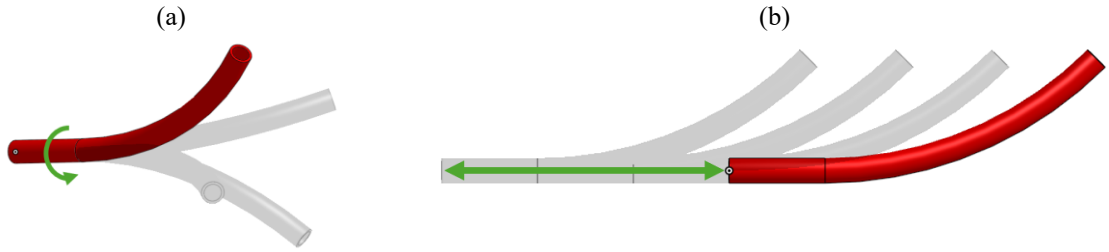

Figure 4. Illustration for 2 DOF of individual nitinol tubes: (a) rotation and (b) translation

On a combined tube, when two curved sections from individual tubes are rotated with respect to one another, the combined curvature changes (Figure 5), which add another degree of freedom to the combined tube.

Figure 5. Rotating two curved tubes within one another changes the curvature, which helps the original tube achieve an additional DOF.

A “controllable curved section” or “controllable curve” is defined as a section in the combined tube where you can control 3 things separately: rotation, translation, and curvature (Figure 4a, b and Figure 5). Two controllable curved sections are considered independent if the three motions of each section are decoupled. By combining individual tubes with different curved and straight sections arrangement, we can create a combined tube with controllable curved sections.

A balanced pair refers to 2 nitinol tubes that, when used together in the whole system, create a controllable curved section where the combined curvature could go from its maximum value down to zero (making a curve become straight). This controllable curved section is controlled by rotating and translating the two nitinol tubes. The stiffness mentioned in this thesis will mean the stiffness of the whole tube structure rather than the material, unless otherwise specified. Bending stiffness refers to the resistance of a tube to a force perpendicular to its longitudinal axis, while torsional stiffness refers to the tube's resistance to torque around its longitudinal axis.

Epipolar geometry is a concept in computer vision that relates 3D objects and 2D images [19]. Using a checkerboard pattern, one can calculate the extrinsic matrix (which projects points from the world frame to the camera frame) and the intrinsic matrix (which projects points from the camera frame to the image frame).

Projection matrices (calculatable from intrinsic and extrinsic matrices) are projections from a 3D frame to a 2D image and can be used to reconstruct 3D coordinates from 2D coordinates on the image. When a 3D point appears in one image, its position on the second image must lie on an epipolar line. The intersection of these epipolar lines is called an epipole. The fundamental matrix relates the coordinates of the same points in two images and is used to calculate the epipolar line. When tracking is mentioned in this thesis, it means tracking of the tubes, not the actuation system.

Robot operation system 2 (ROS 2) [20] is an open source framework for developing robotics software. It uses concepts such as publishers and subscribers for communicating between nodes in a distributed control system. RViz is a ROS package and is used for visualizing the 3D data [21]. In RViz, point cloud represent a collection of 3D points and is used for visualizing the 3D coordinates of CTR in this project.

To ensure accessibility for future research projects, we exclusively used open-source software. Additionally, all parts and procedures were selected and designed so that they could be easily purchased or performed by industrial partners. Except for the nitinol tubes (which were available in advance) and laser-machine step (which was helped by an academic partner), the budget of this project did not exceed £400.

2.2 Design and manufacturing

2.2.1 Rationale for transiting from triplet to quadruplet design

The project initially aims to use 3 tubes to build a CTR with 2 independently controllable curved sections. However, as we progressed, we found that this was not achievable using the balanced pair principle. Although this approach could create two controllable curved sections, the sections are not independent. The proof for this claim is presented below.

To have a controllable curve from a pair of tubes using the balanced pair principle, each tube in the pair must have a curved section that does not overlap with all of the other curved sections from all the other controllable curved sections. To achieve 2 controllable curves with 3 tubes, we will need a total of 4 curved sections on them, leading to at least 1 tube having 2 curve sections (Figure 6a). If we use the balanced pair principle to control this tube, when the other tubes rotate around this one, only the curvature of the two sections can be changed (Figure 6b). On the other hand, the rotation (or twist) of these two curved sections on the same tube cannot be changed (more precisely, it's very difficult to twist two curved sections on one tube) (Figure 6c). Therefore, the curves on the combined tube from these two sections are not independent (their rotational angle is fixed). The proof is still applicable for a general case, if we want to create n controllable curved sections, we will need at least 2n tubes.

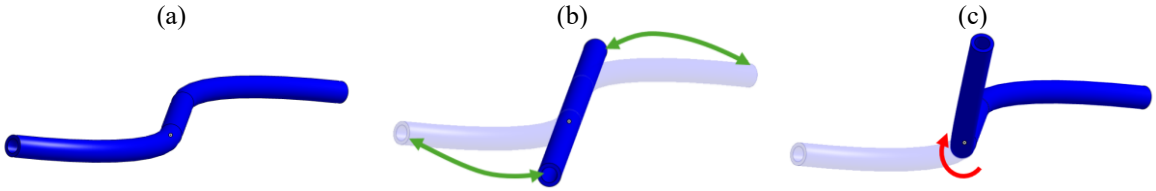

Figure 6. For creating 2 balanced pairs with 3 tubes, 1 tube will have at least 2 curved sections (a). Rotating the other two tubes could only change the curvatures (b), not the relative rotation of the two sections (c).

2.2.2 Design and manufacturing process for balanced pairs

This project used 4 tubes for creating 2 controllable curved sections. The combined tubes are simplified into 1 tube, as illustrated in Figure 3. The tubes were numbered from 1 to 4, with tube 1 being the smallest. The controllable curved section 1 is created from tubes 1 and 2, while the controllable curved section 2 is created from tubes 3 and 4, which is the main target of this project. The tube sizes are given in Table 1.

	Tube 1	Tube 2	Tube 3	Tube 4
Inner diameter (mm)	0.272	0.432	0.75	1.15
Outer diameter (mm)	0.373	0.533	0.95	1.63

Table 1. Tubes sizes.

The arrangement of the curved section as well as their bending stiffness was designed to achieve a tube system with two independently controllable curves. A proposition for the design was that the bending stiffness of a tube could be reduced at will by machining slots on it. FEA was performed to find the best patterns that meet the bending stiffness required. The tubes are then laser cut and heat-shaped to get the desired properties. At the same time, an actuation system for controlling the tubes was developed. Two systems were integrated after that (Figure 7). The details of each step are explained in detail in the subsequent sections. Although the project only focuses on 2 controllable curved sections, all the designs are intended to be modular and can be extended for a higher number of controllable curved sections.

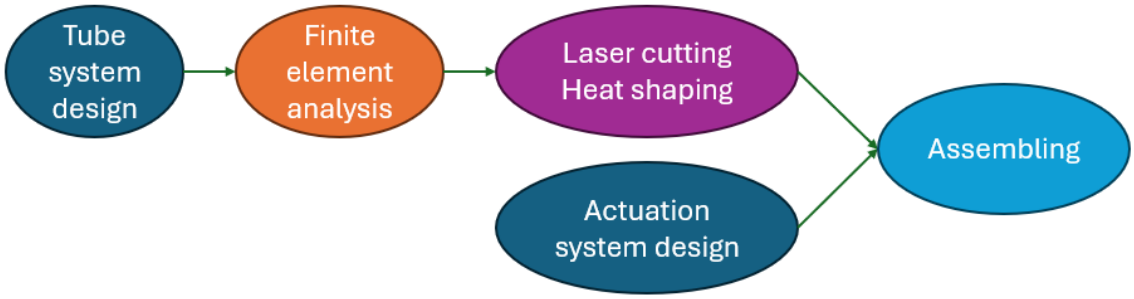

Figure 7. Illustration for design and manufacturing process.

2.2.3 Arrangement of straight and curved sections of the nitinol tube system

For achieving two independently controllable balanced pairs, the nitinol tubes were laser-machined and curved as described in Figure 8.

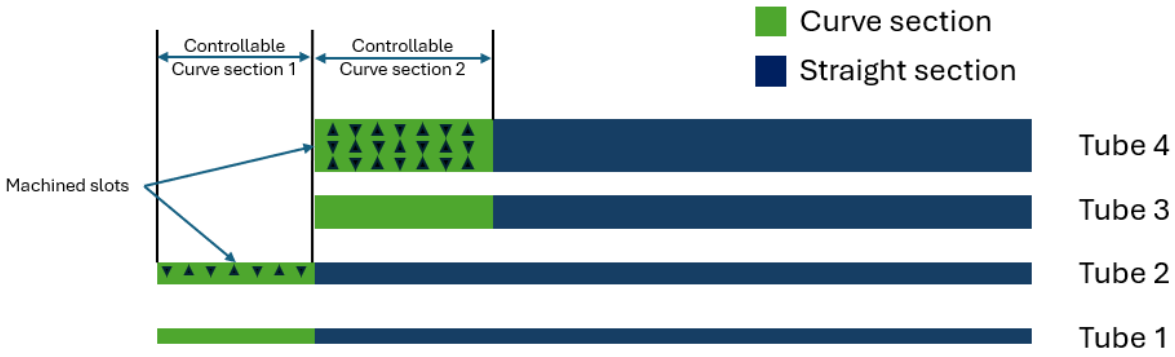

Figure 8. Arrangement of straight and curved sections in nitinol tubes for achieving two independently controllable balanced pairs. Sections with triangles indicate the regions where the tubes were laser-machined.

Each tube was designed to be a straight tube with a curved section of 2 cm at the end. The slots were laser-machined in tube 2 and tube 4 so that the bending stiffness of tube 2 matched tube 1, and the bending stiffness of tube 4 matched a combination of tube 1, 2, and 3.

2.2.4 Slot design and finite element analysis

The slot patterns were designed on the unfolded rectangles of the outer surfaces of tubes 2 and 4. Onshape was used for the design process [22] . These patterns were developed in an isotropic manner, testing various hole sizes, densities, and shapes. FEA was performed using PrePoMax [23] with CalculiX [24] solver. The meshes were generated from the tube's models with a minimum element size of 0.022mm and a maximum element size of 1.1mm. Because the tubes were expected to work in their elastic regions, FEA was performed using a simple linear elastic analysis with Young's modulus of nitinol set to be 50000 MPa. In simulation, tubes of 2 cm with different slot patterns were fixed on one end and received a constant force on the other end. The best patterns were chosen based on the displacements at the tips.

2.2.5 Laser cutting and heat shaping of nitinol tubes

Nitinol tubes 2 and 4 were sent to a partner for cutting with a computer numerical control (CNC) laser cutting laser-machine (Coherent StarCut Tube). The tubes were loaded on a rotator, and the laser cut them following the designed patterns.

After cutting, the nitinol tubes are curved using predefined grooves, and then placed into a ceramic chamber furnace (SNOL 4/900 LSC01) to heat to 540 degrees Celsius for 30 minutes (Figure 9). Subsequently, they were drenched into water at room temperature.

Figure 9. The tubes were fixed in premade grooves before placing the whole setup inside the furnace.

2.2.6 Actuation system design

The system was designed on Onshape and 3D printed with PLA material. Four Dynamixel XL330-M077-T servo motors and one OpenRB-150 microcontroller were chosen because of their sizes and the team's familiarity. Spur gears were selected due to their simplicity for transmitting the torque from the motor to the tubes, with a gear ratio of 5:9 to increase the torque exerted by the motor. Details of the commercial parts are given in Table 2.

Name	Number	Manufacture	Part Number
OpenRB-150	1	Robotis	R-902-0183-000
Dynamixel XL330-M077-T	4	Robotis	R-902-0162-000
20-tooth spur gear – 1 module	4	RS PRO	878-7904
36-tooth spur gear – 1 module	4	RS PRO	521-7578
Bearings	12	Budget	MR106-ZZ-NEU

Table 2. Commercial parts.

As each controllable curved section is built from a balanced pair and each balanced pair is independent from the other pair, the actuation system was designed as one module for each balanced pair (Figure 10).

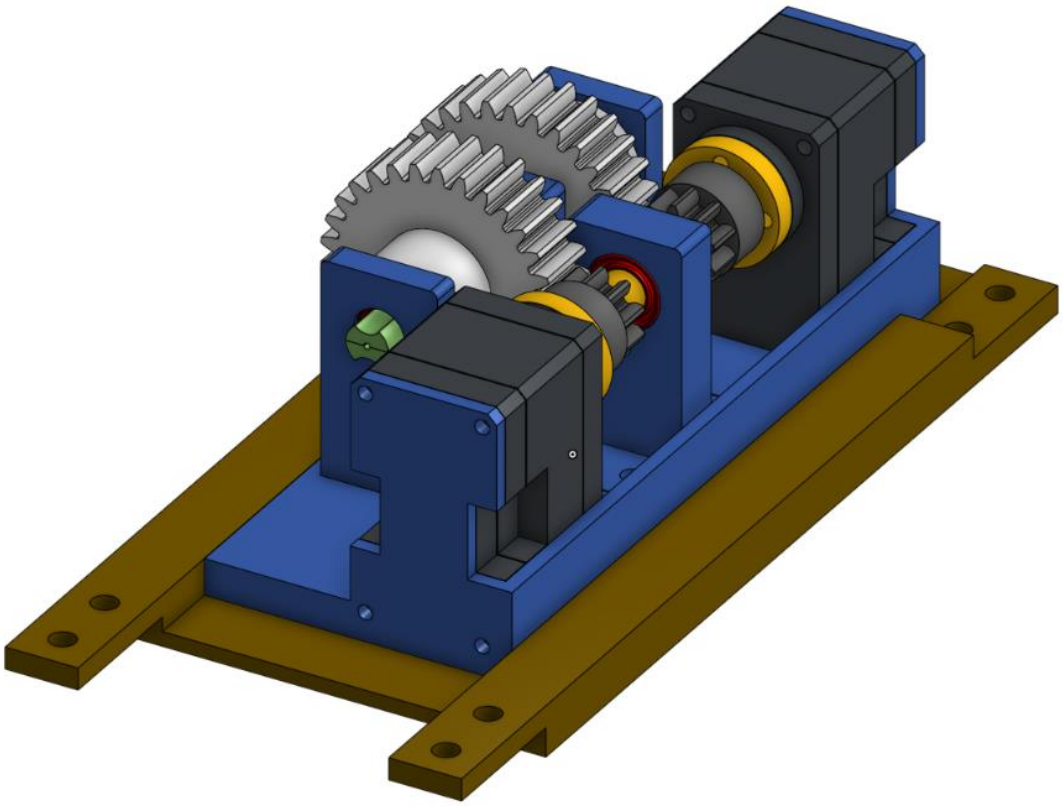

Figure 10. Modular design for the actuation system of one balanced pair.

Each module consisted of two servo motors (black), two motor shafts (yellow), two motor gears (gray), two tube gears (white), two tube shafts (green), six bearings (red), one base (blue), and a slider (brown). In the design, motor shafts were fixed to the motor. The 20-tooth spur gears (motor gears) were fixed to that shaft. The gears then transmitted the rotational torques to 36-tooth gears (tube gears). The tube gears were connected to the tube system through 3D printed tube shafts. The stainless-steel tubes were then connected to the nitinol tubes with epoxy glue to transmit the rotation and translation power. The base supported the rotation of motor shafts and tube shafts with help from six bearings. The whole system was put on a slider to add an extra translational DOF for each balanced pair. An illustration for the CTR after assembling is given in Figure 11.

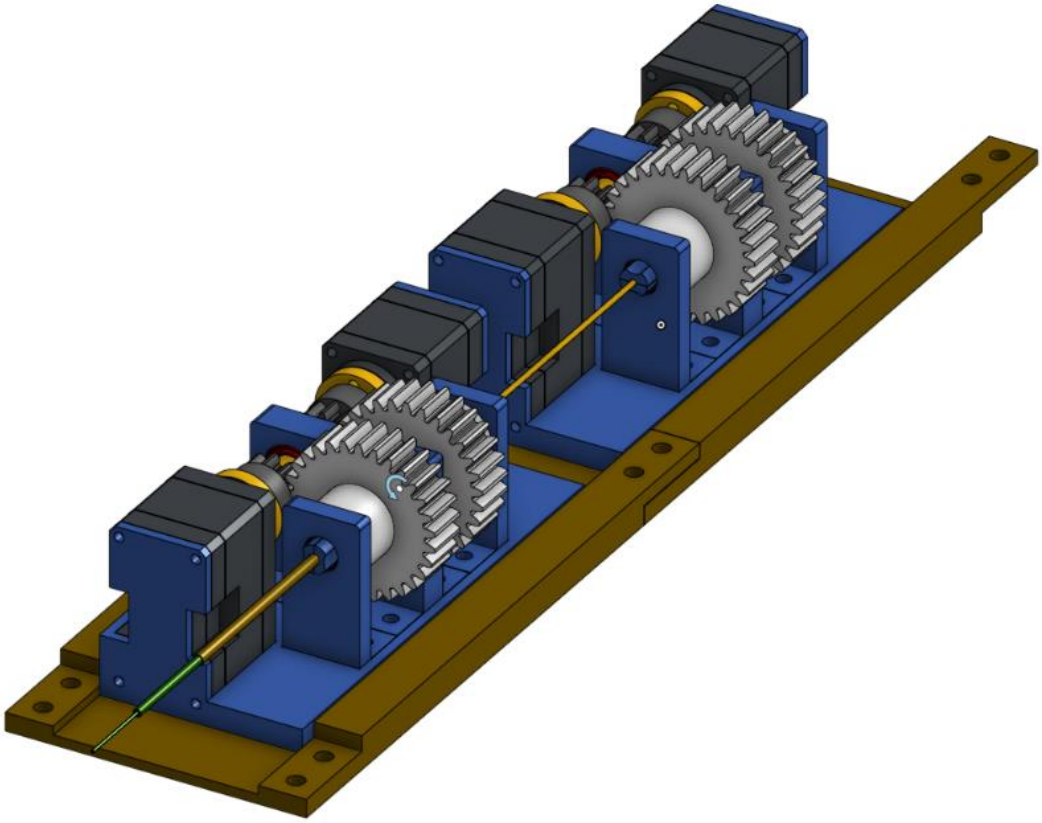

Figure 11. Virtual assembling of the actuation system for a CTR with 2 balanced pairs.

2.2.7 Tube system and its assembly to the actuation system

Stainless-steel tubes were used to connect to the nitinol tube to extend their length so that they could reach the tube shafts (which were fixed to the tube gears) (Figure 12).

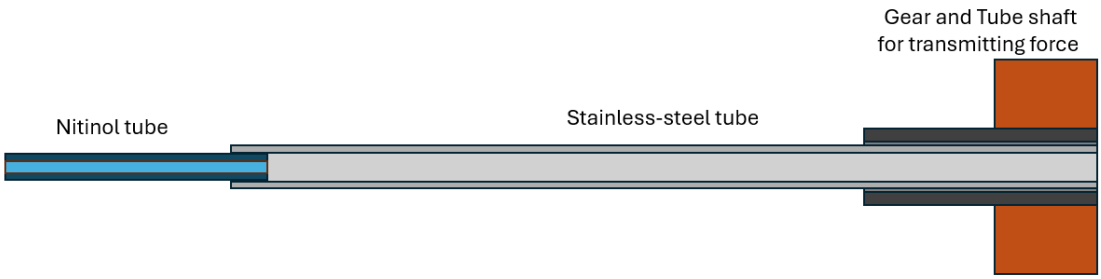

Figure 12. Connection of the nitinol tube to the main actuation system for 1 tube.

The stainless-steel tubes were glued with the nitinol tube and tube shaft using epoxy glue. The glueing started with smaller tubes, bigger ones are nested and glued one by one. The arrangement of the whole system is given in Figure 13.

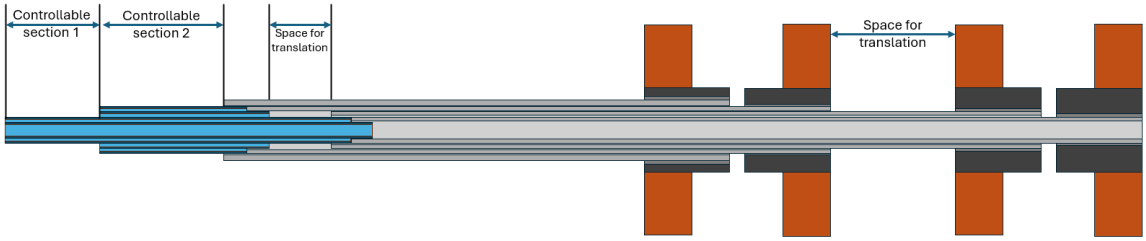

Figure 13. Nitinol tubes and stainless-steel tubes arrangement and connection.

For assembling into the system, the lengths of the stainless-steel tubes and nitinol tubes were calculated based on the design and is given in Table 3.

	Length		Length
Nititnol tube 1	54 mm	Stainless steel tube 1	203.8 mm
Nititnol tube 2	50 mm	Stainless steel tube 2	177.8 mm
Nititnol tube 3	30 mm	Stainless steel tube 3	96.8 mm
Nititnol tube 4	26 mm	Stainless steel tube 4	70.8 mm

Table 3. Length of the nitinol and stainless-steel tubes.

2.2.8 Validation

The nitinol tubes were fixed at one end and subjected to tension using a digital force gauge at the other end. Displacement was measured with a ruler for preliminary estimation and compared with FEA results.

The first balanced pairs were evaluated by nesting the curved section of tube 1 and tube 2. Their curvature was assessed visually when the tubes were rotated in the same direction and in opposite directions as described in Figure 4. The second balanced pair were evaluated by rotating tube 4 around a combination of tubes 1, 2, and 3. Similarly, the curvature was visually inspected when they were rotated in the same and opposite directions.

The assembled system was then evaluated for the decoupling of the controllable section 2 with respect to controllable section 1 by trying different rotation, curvature, and translation of the second section.

In post-hoc analysis, we investigated the impact of different curvatures of individual tubes on the balance pair. Copies of nitinol tube 2 were curved at different curvatures and rotated within the same nitinol tube 1.

2.3 Stereo tracking system

2.3.1 Setting up and tracking protocols

The CTR was tracked with two commercial mini-USB camera boards. A frame was assembled from aluminum profiles to fix the camera, and camera holders were CAD designed and 3D printed to connect the camera with the frame. The camera holders were designed so the camera angles can be easily changed in the future. As we expected the camera systems to be integrated into the control system of the CTR in the future, ROS 2 was used as a framework for running the segmentation and 3D reconstruction algorithms.

The algorithm was implemented using OpenCV library [25] as one ROS node on a Linux computer. In every cycle, the algorithm iteratively go through each camera. Before starting the loop, the cameras are

calibrated to get their relative 3D position; the background and the color of the CTR are registered and used as references for segmentation in the main loop. In the main iteration, the cameras segment the tubes from the background (segmentation), and then, for each point on the first camera image, it find a corresponding points on the second camera (stereo matching). The matched points are then used to reconstruct 3D coordinates of the tube (3D reconstruction). The coordinates are published to RViz for visualization. A summary of the steps can be found in Figure 14.

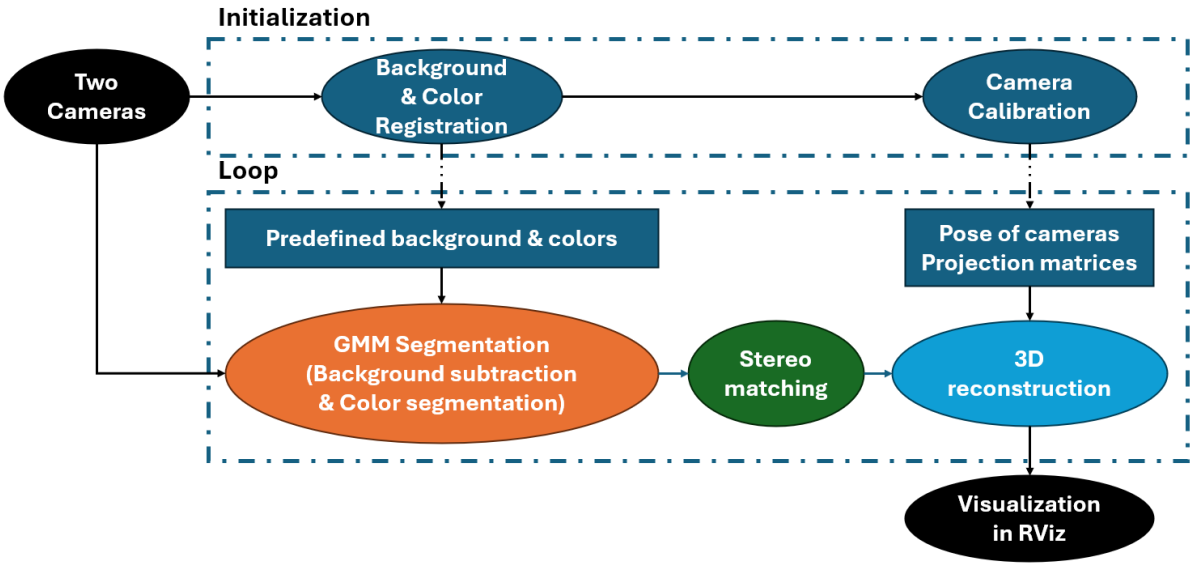

Figure 14. Protocols for 3D tracking of the CTR.

2.3.2 Camera calibration

After a 6x4 checkerboard with a 15mm edge was placed before two cameras, the checkerboard corners were detected with cv2.findChessboardCorners function. The 3D coordinates of these corners (which are known from the checkerboard dimension) were used together with the 2D coordinates of the detected corners on the image to get the internal and external matrices with cv2.calibrateCamera. These are used to calculate the projection matrices. The fundamental matrix was calculated from the detected corner using cv2.findFundamentalMat.

2.3.3 Segmentation

To increase the robustness of segmentation, two techniques were combined: background subtraction and color segmentation. In the initialization, the background is registered (with no CTR in the view), followed by the registration of the colors of the tubes. In the main loop, segmentation was performed using a gaussian mixture model (GMM) approach to classify the pixels [26] with the built-in function cv2.createBackgroundSubtractorMOG2. This technique fits a GMM for each pixel, returning a probability of a pixel being the background and matching the register color. The probability cut-offs for classification were tuned based on experience. The segmented images are visualized as a binary map, where the pixels are 1 if it is not a background and it matches the registered colors.

2.3.4 Stereo matching and 3D reconstruction

The 2D coordinates of those active pixels on the segmented image are extracted and used for stereo matching. For each point in the first image, the algorithm uses the fundamental matrix to calculate a corresponding epipolar line on the second image using cv2.computeCorrespondEpilines. It then identifies a collection of active pixels on this line and selects the center point to create a pair of matched points. For simplicity, if the algorithm finds two collections of active pixels on the lines, it will not use that pair for 3D reconstruction.

Pairs of matched points are used to calculate the 3D coordinates of CTR using the projection matrices with cv2.triangulatePoints. The node then converts these coordinates into a cloud point and publishes them to RVIZ in ROS 2.

2.3.5 Validation

The algorithm was evaluated when changing the tube configuration under the camera and evaluating the update frequency (calculated as the inversion of the time for each 3D reconstruction). The segmentation and 3D reconstruction performance were evaluated subjectively by visually comparing the algorithm's results with the ground truth.

3 RESULTS

3.1 Design and manufacturing outcome

3.1.1 Final slot patterns and finite element analysis results

The FEA software execution time went up to two minutes when simulating multiple tubes with different slot patterns at the same time. Over 2 cm pieces of tubes, we tested three different patterns and investigated how they impact the overall stiffness in FEA (Figure 15).

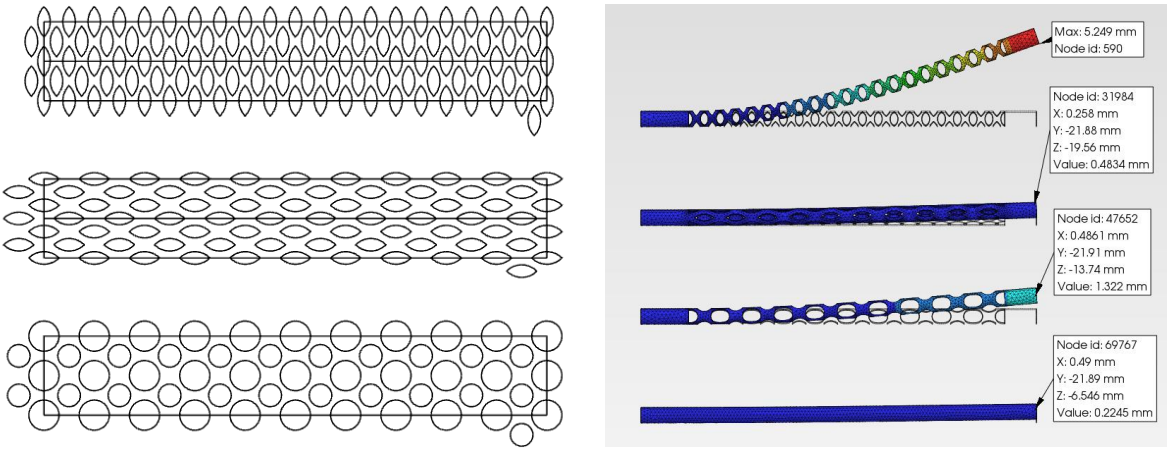

Figure 15. Three slot patterns that were compared. The tubes were unfolded into rectangles with a height of 20 mm and a width equal to the outer circumference of nitinol tubes. The laser cutter followed the path within this rectangle. The first pattern involves circles of different sizes, while the others involve intersections of two circles. The patterns were arranged to increase the portions of materials that would be removed using that pattern while maintaining the minimum distance between two slots at least 0.15 mm. Force of 0.05 N.

We found that, by using a cutting pattern having a width greater than height, we can increase the density of the slots as well as significantly reduce the bending stiffness of the tubes. Therefore, for the rest of the project, we used ellipses with a major axis perpendicular to the longitudinal axis as the main pattern and mostly tuned for the ellipse axis length and the pattern repetition.

The first balanced pair was created by comparing the first tube with the machined second tube in FEA when fixing one end and applying 0.05N on the other end. The displacement of tube 1 was 5.436 mm. Different ellipse patterns were tested for tube 2, and the pattern that resulted in 5.01 mm displacement was chosen (Figure 16).

(a)

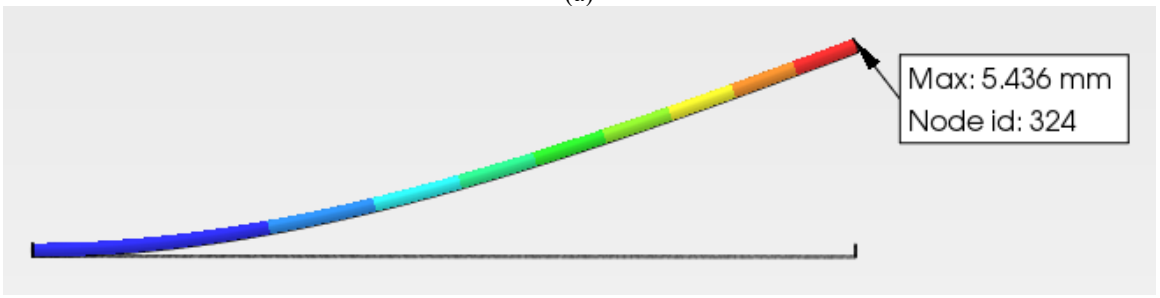

(b)

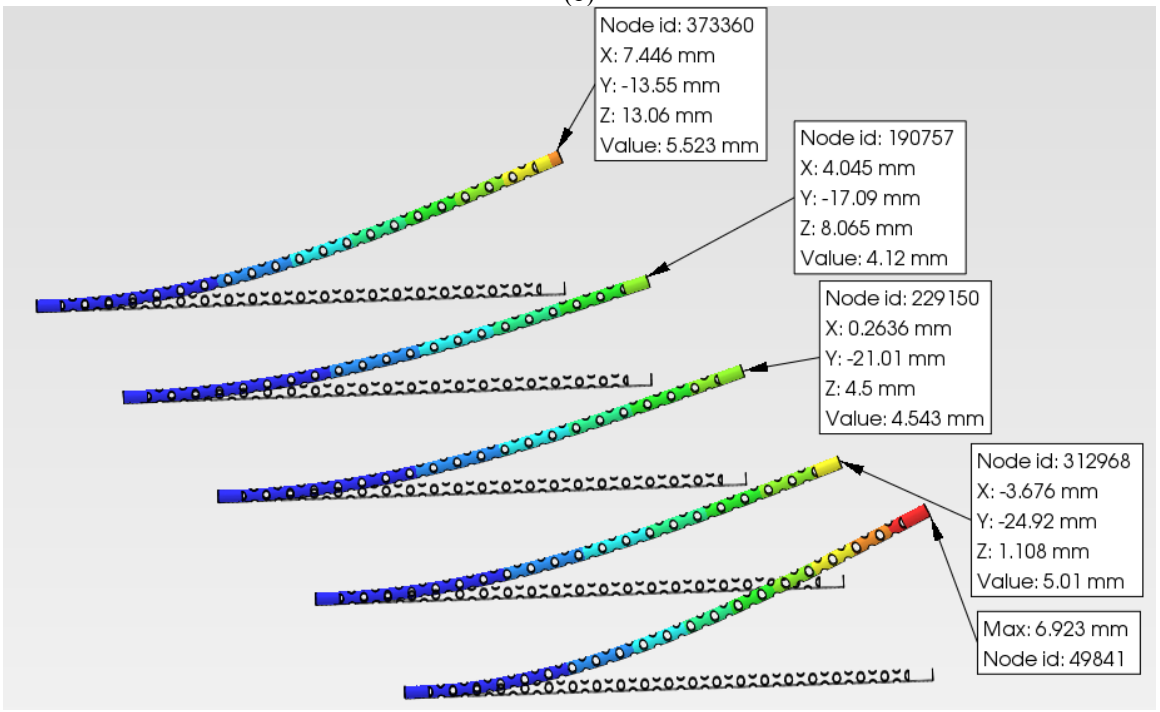

Figure 16. FEA for the first controllable curved section for (a) tube 1 and (b) tube 2. The tubes were fixed to one size and received a 0.05N on the other size. Different sizes of ellipse were tested as slot patterns for tube 2.

Similarly, the second balanced pair was created by comparing the combination of tubes 1, 2, and 3 with the laser-machined tube 4. The force used was 2N. The displacement of the combination of tubes 1-3 was 5.479 mm. The ellipse pattern resulting in a displacement of 5.262 mm was selected for tube 4 (Figure 17).

(a)

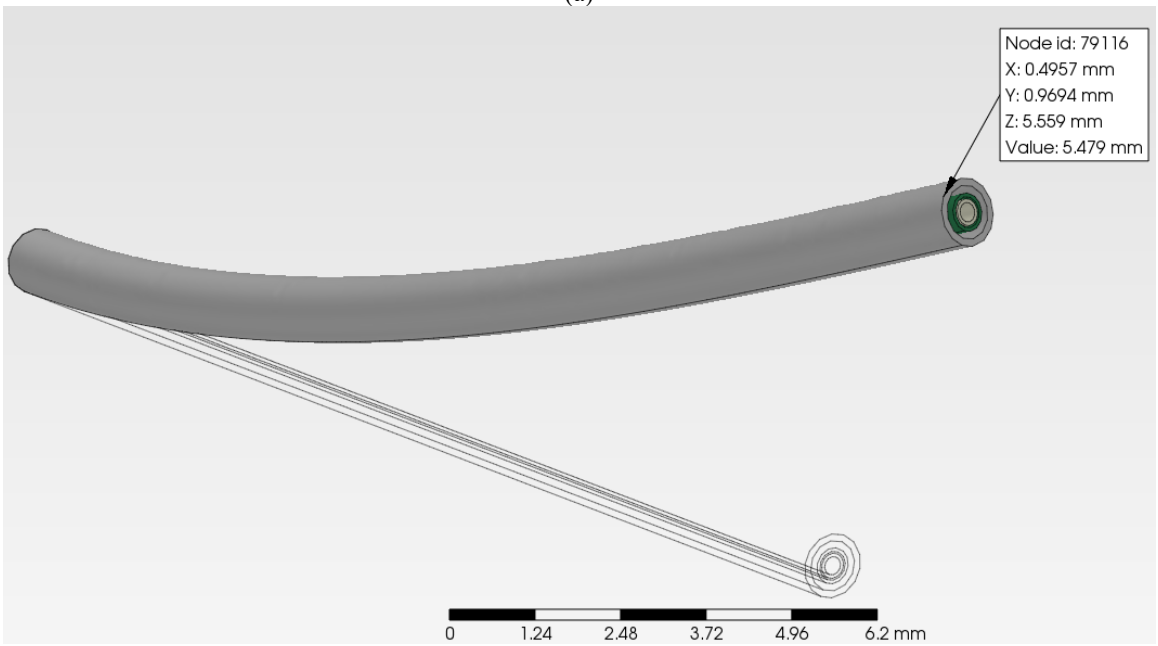

(b)

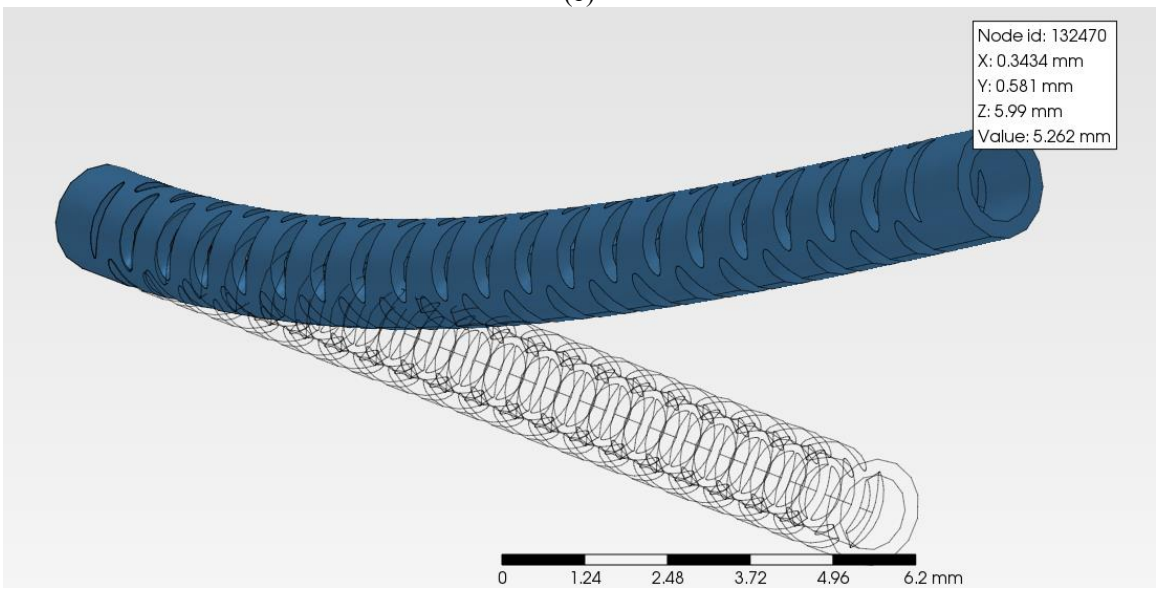

Figure 17. FEA for the second controllable curved section for (a) combined tubes 1-3 and (b) tube 4. The tubes were fixed on one size and received a 2N on the other size.

The final patterns for tube 2 and tube 4 are given in Figure 18, with tube 2 slots constituted of ellipses with axes of 0.23mm and 0.15mm, and tube 4 slots comprising ellipses with axes of 0.69mm and 0.20mm. The ellipses were repeated twice over the horizontal axis and 40 times over the longitudinal axis.

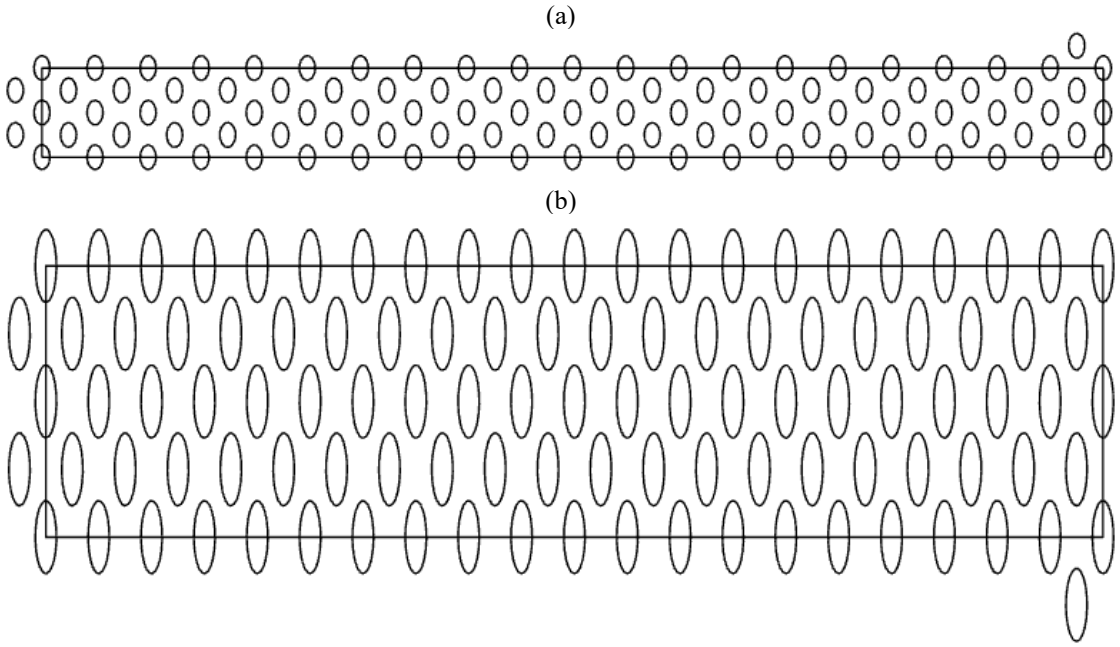

Figure 18. Final slot patterns for tube 2 and tube 4 and their FEA result.

3.1.2 Balanced pairs evaluation

While tube 2 was easily sliced with the laser cutter, it barely went through tube 4. Therefore, the final samples consisted of four tubes 2 and one tube 4. Experiments were done to compare the real displacement of nitinol tubes with FEA results (Table 4).

Tube	Force	FEA displacement	Experimental displacement
1	0.05 N	5.436mm	6.5±0.5mm
2	0.05 N	5.01mm	6.5±0.5mm
3	1.0 N	3.076 mm	5.5±0.5mm
4	2.0 N	5.262 mm	7.5±0.5mm

Table 4. Comparison of FEA results and experiment results. The FEA for Tube 3 was conducted later to compare with experimental data. The experimental displacement is presented with an uncertainty of ±0.5 mm.

The average difference between FEA simulation and experiment was about 1.8 mm. This was a significant number, as it was equal to 38% of the average displacement of the FEA simulation. However, these results should be interpreted with care, as they were only preliminary estimations with a ruler. A picture of the laser-machined tubes under a microscope is given in Figure 19.

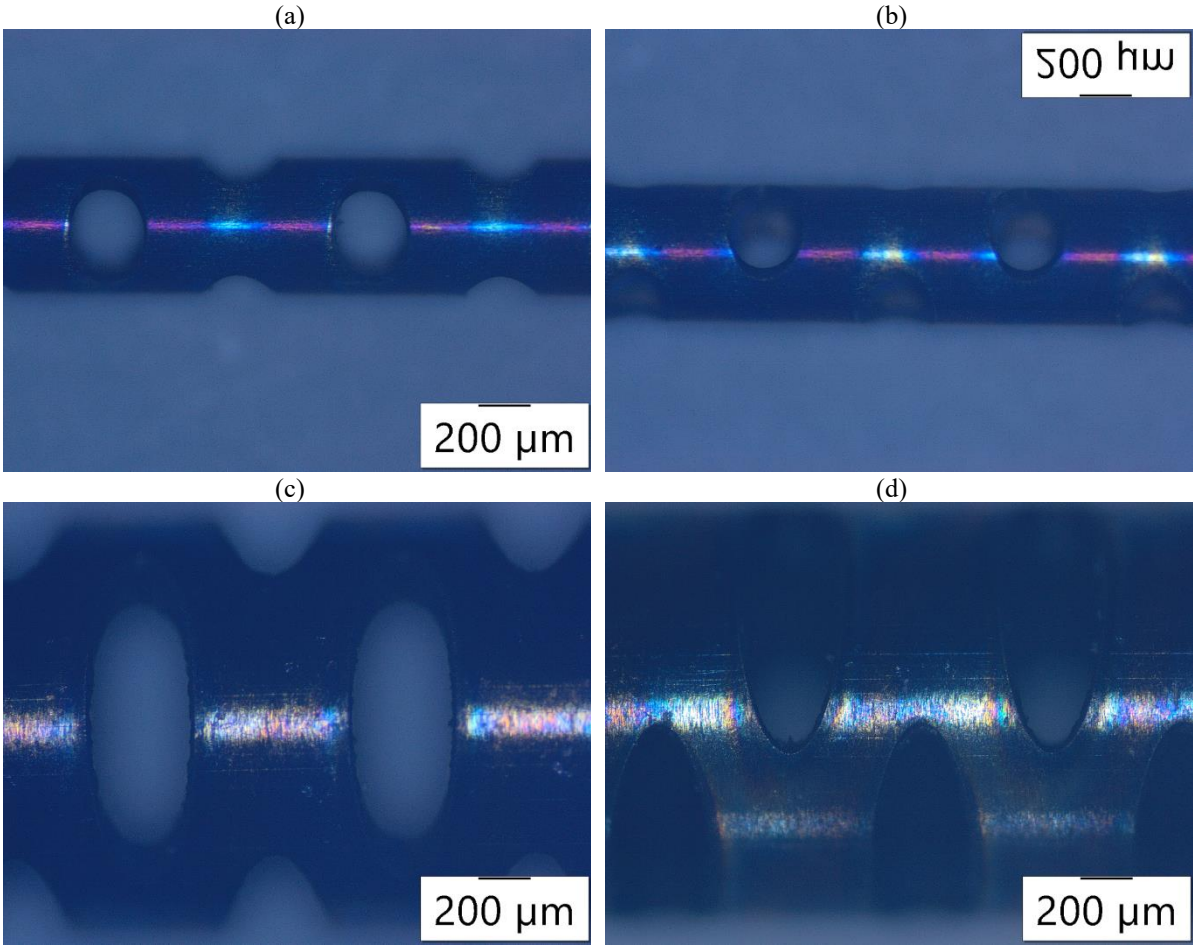

Figure 19. Images under a microscope of tubes 2 (a), (b), and tube 4 (c), (d).

Balance pair 1 was tested by nesting tubes 1 and 2 in the same and opposite directions. When they were rotated in the same direction, the combined section was curved. When they were rotated in the opposite direction, the combined section became straight (Figure 20a and 20b). In testing balance pair 2, a similar result was observed (Figure 20c and 20d). This indicated a success for the designed slots.

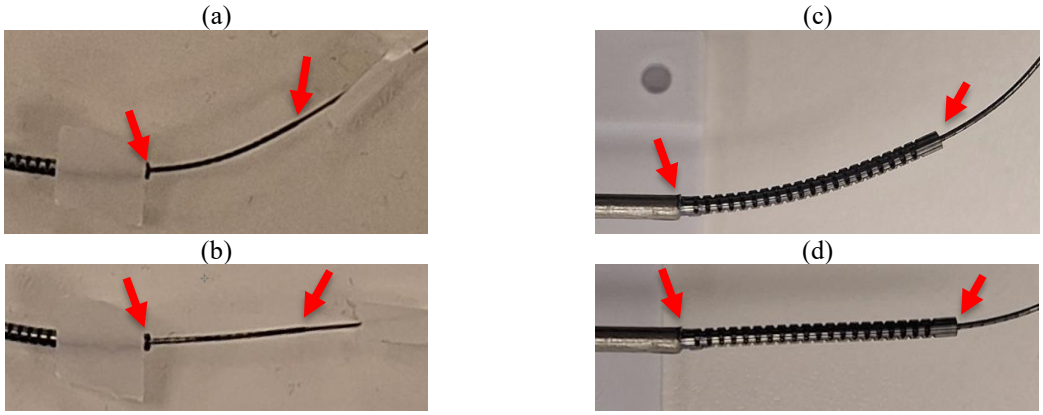

Figure 20. Tube 1 was nested within tube 2 when they were rotated in the same direction (a) and opposite direction (b). The combination of tubes 1, 2, and 3 was nested within tube 4 when they were rotated in the same direction (c) and opposite direction (d). The red arrows point to the start and the end of the balanced pairs.

3.1.3 Actuation system

The dimensions of each module were 10.2 x 6.3 x 3.8 cm (length x width x height). And the total length of the whole system is 21.7 cm (not considering the tubes). Unfortunately, the diameter and tolerance of stainless-steel tube 1 were miscalculated, and its inner diameter was too small to be able to fit the outer diameter of nitinol tube 1. Due to time constraints, tube 1 was connected directly to the tube shaft instead (Figure 21).

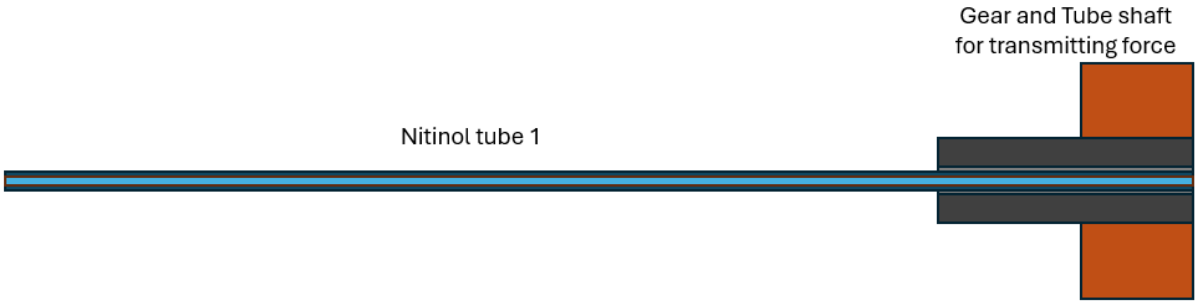

Figure 21. Temporary fix for connecting nitinol tube 1 as the inner diameter of stainless-steel tube 1 was too small to fit the outer diameter of the nitinol tube

The final assembly is given in Figure 22.

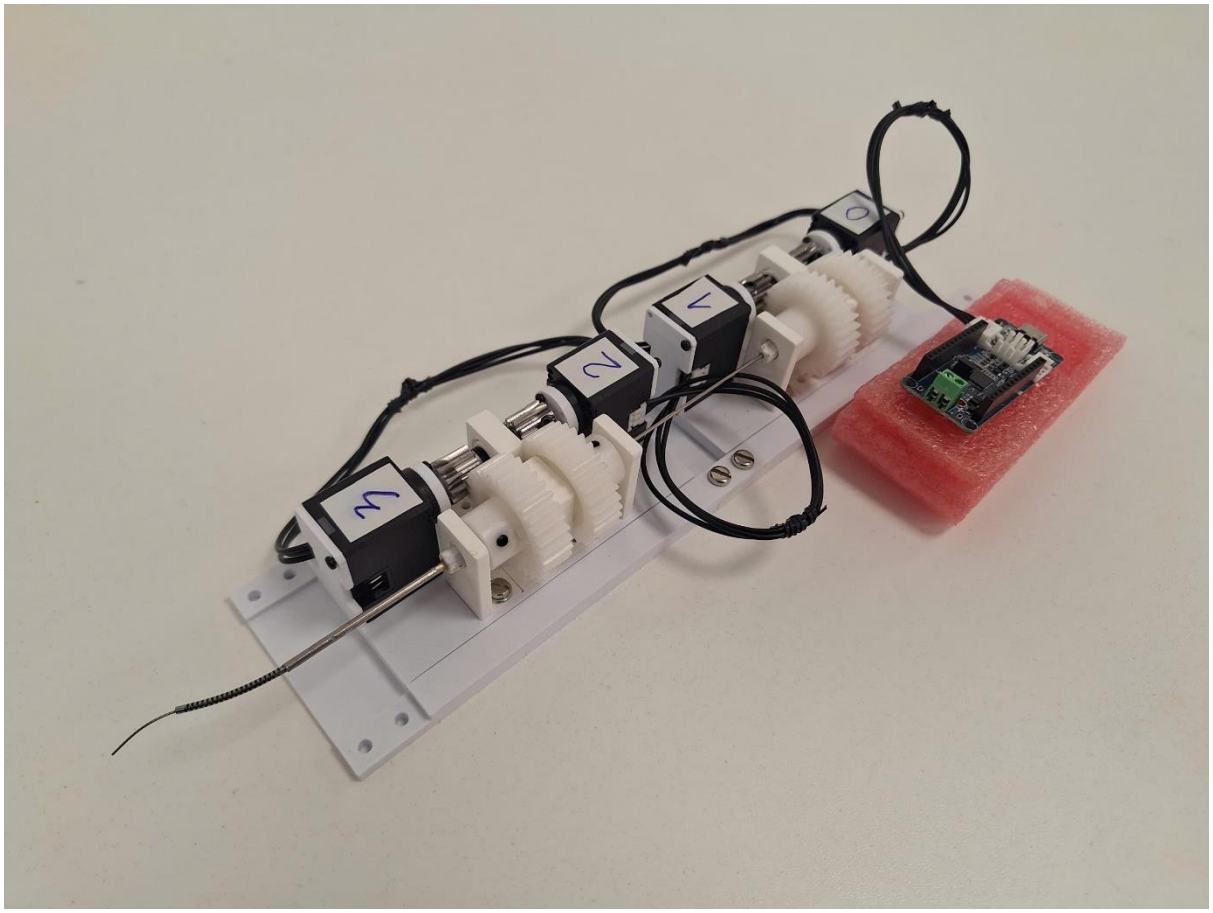

Figure 22. Final assembly of the whole system.

3.1.4 Decoupling of two controllable curves

The second controllable curves section was fully decoupled from the first controllable curved suction (Figure 23). The rotations of the curve created by the second balanced pair were independent of the first curve (Figures 23a, b, c). Its curvature could be changed without affecting the first curve (Figures 23c, d, e, and f). Furthermore, the second balanced pair could be translated without impacting the first one (Figures 23c, d, e, and f).

(a) (b)

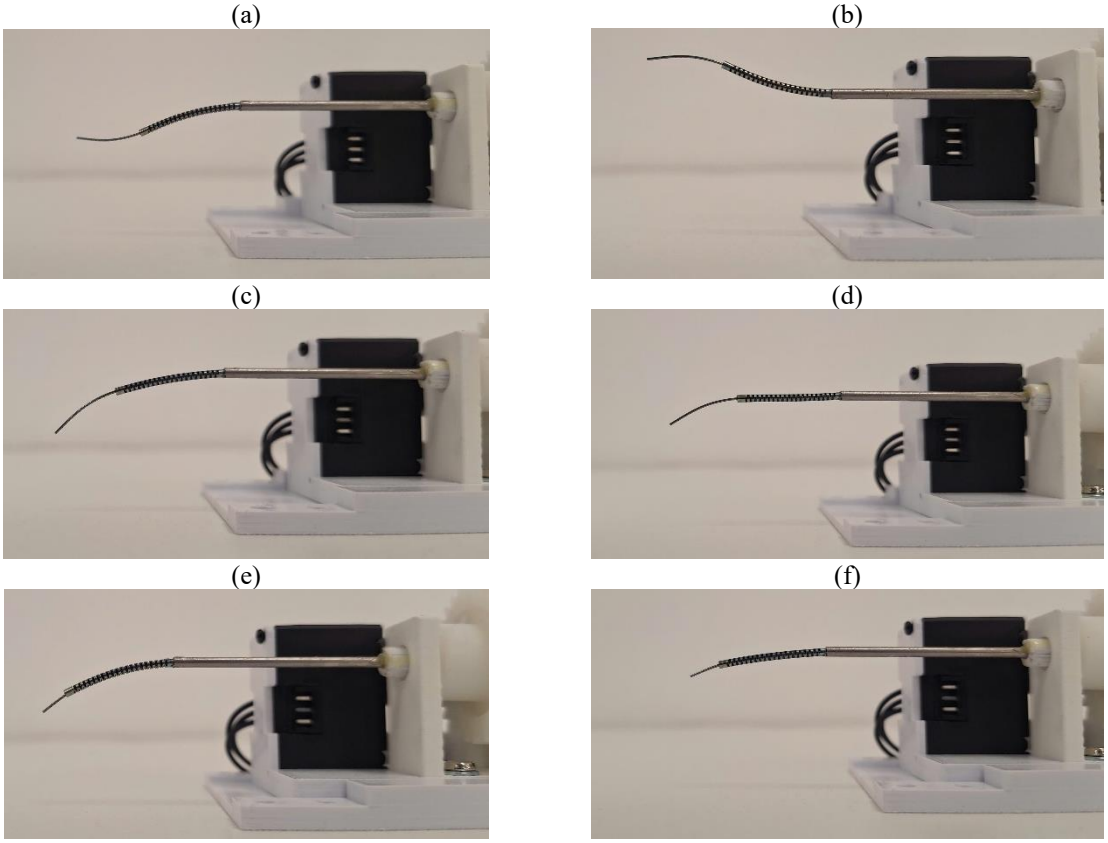

(c) (d)

(e) (f)

Figure 23. Investigation of the decoupling of controllable curve 2 with respect to controllable curve 1 with different rotations (a), (b), (c); curvatures and translations (c), (d), (e), (f).

3.1.5 Impact of different curvature to the balanced pairs.

In a post-hoc analysis, another three laser-machined tubes 2 were curved with a different curvature compared to tube 1 (Figure 24). Two tubes on the left are less curved than the final tube 2 above, and one on the right has a higher curvature.

(a) (b)

Figure 24. Copies of laser-machined tube 2 with different curvature and final curved tube 1.

When tube 2 was curved less than the optimal curvature, the rotational direction of the combined section always follows the rotational direction of tube 1 (Figure 25 a, b) even in the opposite direction (Figure 25 c). On the other hand, when tube 2 was curved more than the optimal curvature, it followed the rotational direction of tube 2 (Figure 25 d, e). This suggested that, if the slot designs are not optimal, and the initial pair is not balanced, we can tune the curvature of the nitinol tube with heat shaping to achieve a balanced pair instead of redesigning and machining new pairs.

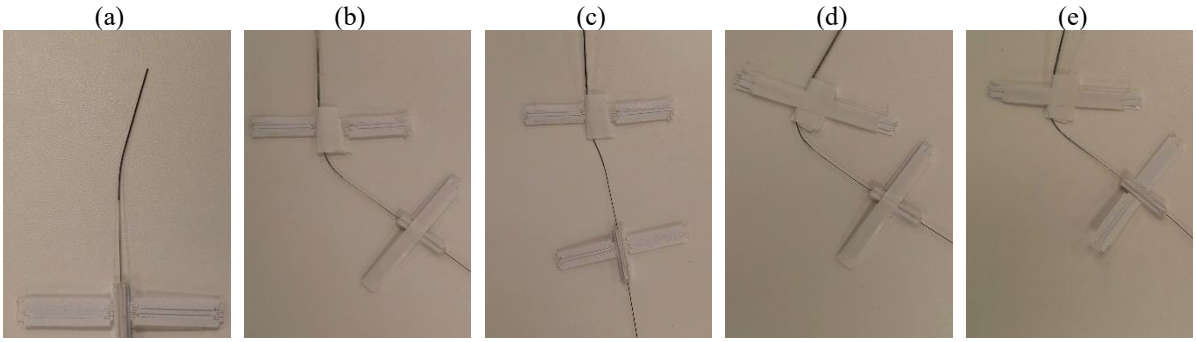

Figure 25. A same curved tube 1 was nested and rotated within copies of nitinol tube 2 of different curvature: (a) straight tube 2; (b, c) tube 2 with a less curvature in the same and opposite rotational directions, respectively; (d, e) tube 2 with a higher curvature in the same and opposite directions, respectively. In (c) and (e), tube 1 was rotated 180 degrees. The white tape and plastics help limit the rotation of the tube and are not fixed to the tables.

3.2 Performance of stereo tracking system

3.2.1 Tracking system

The camera holder design and the final setup are given in Figure 26.

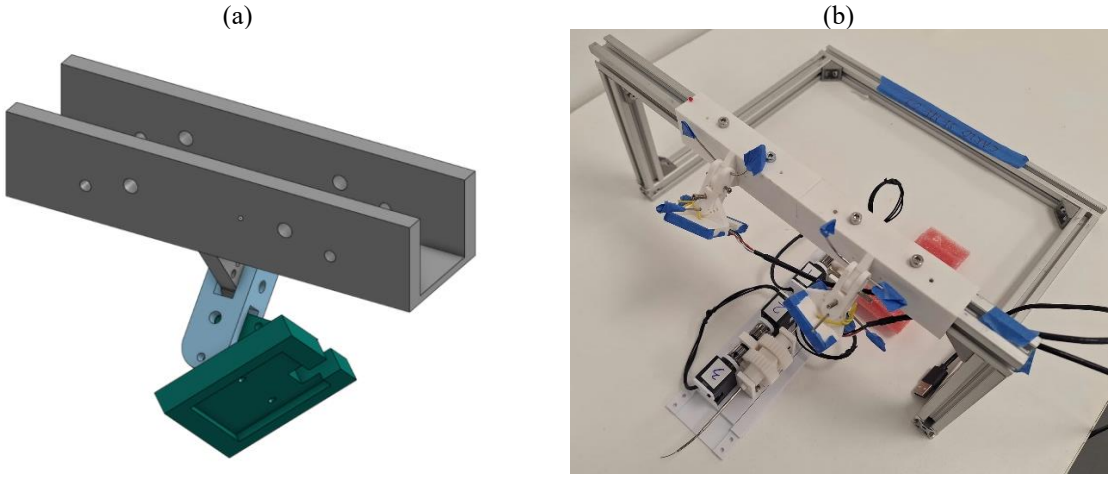

Figure 26. Design of the camera holders (a) and the final setup (b).

3.2.2 Segmentation and 3D reconstruction performance

The segmentation algorithm required the cameras to be fixed, yet it performed well and successfully

extracted the CTR without needing to control the lighting conditions (Figure 27).

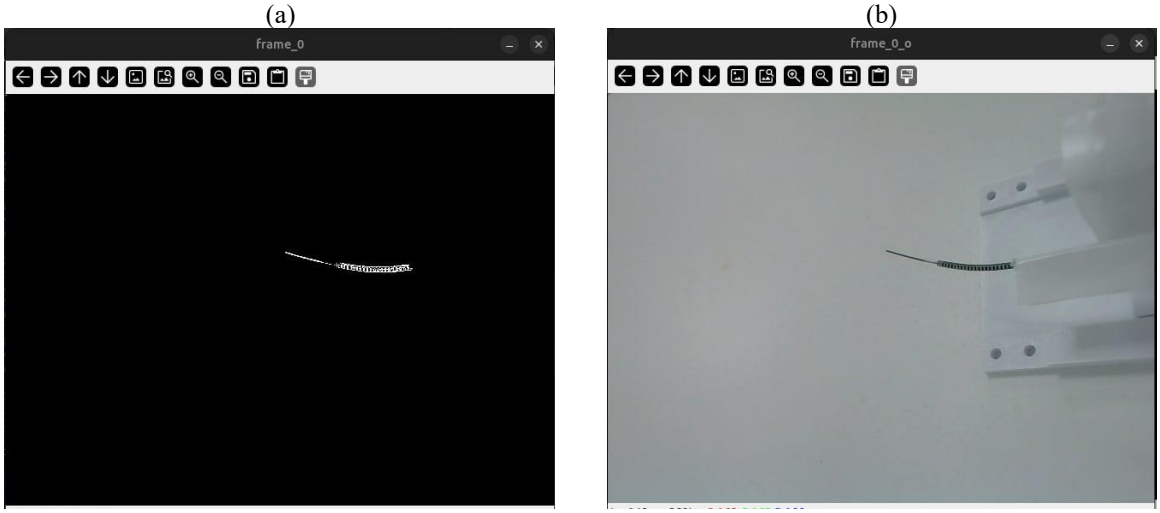

Figure 27. Performance of segmentation (a) and ground truth (b).

The 3D reconstruction was also implemented well with an update frequency of 8Hz (0.12s±0.01 for each 3D reconstruction). The algorithm could catch the orientation as well as the position of the entire tube Figure 28.

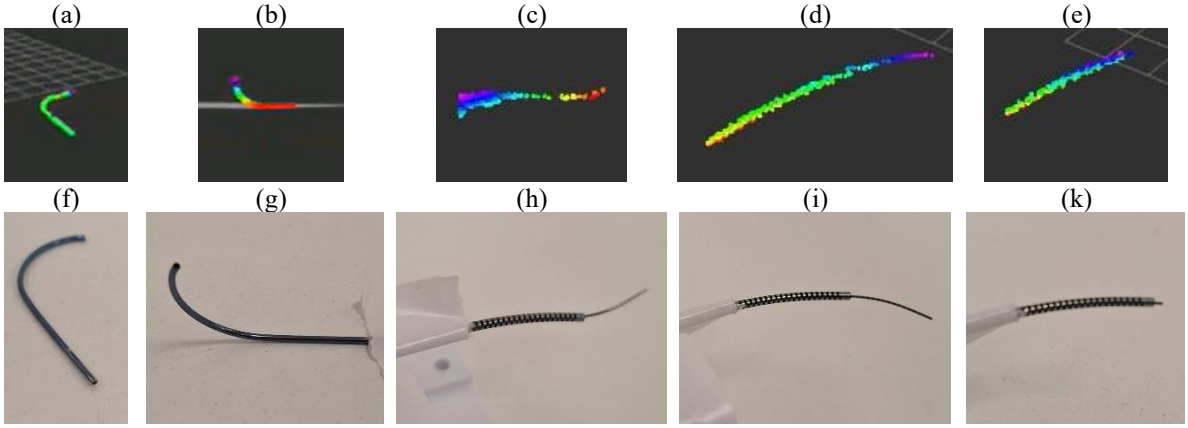

Figure 28. 3D segmentation performance. Segmentation performance (a), (b), (c), (d), (e), and their corresponding ground true (f), (g), (h), (i), (k).

The system can trace the translation of the CTR. However, it struggled to detect subtle changes in rotation and curvature, which might be due to the oversimplification of the approach.

4 DISCUSSION

4.1 Summaries, interpretation, and recommendations

The project successfully created an original design for achieving a second balanced pair that can be controlled independently from the first pair as well as developed a novel 3D stereo tracking system for comprehensive monitoring the entire CTR. We proved theoretically that a system with 2 controllable curved sections using the balanced pair principle is not achievable with less than 4 tubes. This proof also generalized – a system with n controllable curved sections using the same mechanism will need at least 2n tubes.

A key advantage in our work is the modular approach for each balanced pair in both the design and

manufacturing process. This makes it theoretically possible to get a CTR with 3 or more controllable curved sections. The tube system can be extended by adding pairs of bigger nitinol tubes outside the current tubes, following the same principle, while each module in the actuation system can be simply replicated in the process of adding more controllable sections. However, it is worth mentioning that the real implementation will depend on the problems, and its feasibility will need to be tested case by case. When using the same design, as the number of controllable curved sections increases, the largest nitinol tube needs to be bigger, and the smallest nitinol tube needs to be longer. Bigger nitinol tubes require motors with higher torque to control the curvature, while longer tubes increase the risk of snapping as it reduces the torsional stiffness and increases the BTSR [11].

Our FEA setup turned out to be a good one for simulating and selecting the best slot patterns for creating balanced pairs. Calculix is an open-source software, making it easily accessible to research groups. The simulation was simple, and the time executed was only 1-2 minutes, making the process of tuning multiple slot designs fast and easy. We also found that, for our approach, simple slots of oval shapes in an isotropic would work well for reducing the bending stiffness, even though researchers have tried to increase the stability of CTR using anisotropic slot patterns [9], [10]. This might be because the lengths of the nitinol tubes in our approach were small due to using stainless-steel tubes for extension, which reduced the torsional stiffness of the nitinol tubes. Additionally, the results indicated that placing the major axis of the oval perpendicular to the longitudinal axis of the tubes reduces the bending stiffness the most. In our tuning process, we mostly change the size of the major axis; therefore, future projects can start with our patterns and tune the major axis of the oval and change the other parameters (number of repetitions in height and width, size of the minor axis). This will help accelerate the design and tuning process.

In manufacturing the 4th tube, although we got one sample at the end, the laser cutter barely cut through the tube as the wall was very thick, which led to waste of some materials. Therefore, other CNC methods besides laser are recommended for future fabrication if the nitinol tubes are too thick.

The dimension of a miniaturized CTR actuation system designed by Farooq et al. was 26 × 7 × 8 cm [27]. The whole dimension of our actuation system is 21.7 x 6.3 x 3.8 cm, which is more compact. Using the stainless-steel tube allowed extension of our system in the length dimension instead of the width compared to their paper.

The post-hoc analysis of the impact of the degree of curvature on the combined section implied that we could increase the curvature of the tube with smaller bending stiffness and vice versa to create a balanced pair. This offers a more efficient approach than redesigning and machining the nitinol tubes, as we can heat and reshape the nitinol tube multiple times. Future projects could create a balanced pair by first doing a simple design and FEA and then tuning the curvature of the nitinol tube to create a balanced pair.

Our simplification of the CTR into 1D shapes of arcs and straight lines might be a viable approach when we want to use the balanced pair principle for controlling. Each controllable section can be thought of as an arc of length l and a curvature of c (where c equals the inversion of the radius of the arc). The arc can be translated a distance of d and rotated through an angle of θ. A controllable curved section will have three degrees of freedom: rotation, translation, and curvature, which corresponds to θ, d, and c. Rotational angles θ range from $-\pi$ to π, translation distance ranges from d_{min} to d_{max}, and curvature ranges from c_{min} to c_{max} ($c_{min} = 0$ if it is a

balanced pair). Based on each task specification, researchers can use this simplification to determine the value of l, d_{min}, d_{max}, and c_{max} so that their CTR could reach the target task space. Additionally, a control system can be designed so that the user directly controls the θ, d, and c instead of the rotation and translation of each individual tube. This will provide users with a more intuitive interface.

Another thing that is worth discussing is the plastic deformation of the balanced pair. As nitinol has a wide elastic region, we did not observe any permanent deformation. However, if future projects require a high change in the curvature c, it might be beneficial to employ a more advanced FEA technique to determine the maximum allowable change of curvature. In such cases, the pair might be designed a little "imbalanced" so that the difference between c_{max} and c_{min} remains within the elastic region.

Regarding the 3D tracking, we proved that, by using a stereo system with two commercial cameras, we can effectively track the whole CTR, which is a very economical approach. Although we only used a middle-tier computer for running the algorithm, it still updated with a frequency of 8 Hz, indicating a potential for real-time application. In the segmentation, while we placed the CTR in a white background, no effort was made to control the lightning or the tube color and reflection. Even so, our segmentation approach using GMM turned out to be a robust approach method for extracting the CTR.

The main component that is in contact with the patient is the nitinol wires. Research on some sterile processes on nitinol found no change in the sample property before and after sterilization [28]. This offers the system the ability to be reused in multiple cycles. Our proposed approach for creating a balanced pair by reshaping a laser-machined nitinol tube instead of re-machined new patterns will help reduce the waste during manufacturing and reduce its environmental impact.

CTR is a cost-effective solution for eye surgery regarding its potential health benefits. All the software used in the project was open source, and the design was compatible with 3D printing. Even so, the cost could be reduced even further. Mass production methods could replace 3D printing, and the laser cutting process could be replaced with other affordable CNC processes by redesigning and tuning the slot patterns. All the commercial parts (except the nitinol tubes) are cheap and can be purchased in large quantities from many manufacturers, especially thanks to the modular design. Although nitinol tubes are expensive, a substantial portion of the tube system is made from widely available and inexpensive stainless-steel tubes. Moreover, CTR's reusability enhances its long-term value and makes it an economical approach.

4.2 Limitation

The main limitation of the project is that we did not make it in time to tune the parameters and validate it with an eye model to see if the system could reach the desired workspace for optic nerve fenestration. Additionally, in the first balanced pair, we got the wrong size of stainless-steel tube 1. As some components arrived so late, we could not replace them and assemble the final, complete system. And we were not able to test the first controllable curved section in the assembled system. This problem can be fixed by getting a new stainless-steel tube of a suitable size. The 3D design of the actuation system module was also not optimized. Although the length of the whole system is about 22 cm, which is reasonably small, by changing the gears to bevel gears, rotating the motors by 90 degrees, and using smaller gears, the length of each module could be halved, making the system much more compact.

In the stereo tracking system, our 3D reconstruction protocol remains a proof of concept rather than a practical system for real-world usage. This is mainly because we lacked validation for its precision within the given time constraint. The camera system is also not a best-practice stereo vision system, as the cameras are uncalibrated. Changing the setup to a binocular stereo vision system (where the cameras are placed in a known configuration) could offer accuracy up to 0.1 mm or better [29]. The current segmentation algorithm bases on background subtraction and color segmentation; therefore, it will not work in the dynamic environment of a surgical operation. Furthermore, our stereo matching procedure relies on a naïve approach. For each point in the first image, the algorithm searches for one point on the corresponding epipolar line on the second image. This basic technique will not work well if two points on the CTR intersect with an epipolar line. As the tube's diameter increases, the CTR segmentation will be more rectangular-like rather than a single line. This will greatly impact the precision, as we are only interested in the central. With further improvement, the system would be a valuable asset in advanced control like path planning and visual servoing [12], [13].

4.3 Future work

Future work on this system would mainly require completing the whole system and validating its performance on 3D models of the eye for optic nerve fenestration. A new stainless-steel tube 1 of a suitable size should be ordered and then assembled into the tube system. Commercial eye and skull models could be used to check if the CTR could reach the target workspace, and the parameters of the CTR could be tuned accordingly. Then, opinions from surgeons should be collected to improve the system. Another topic that could be researched for this system is the control interface. Right now, users steer the CTR by rotating and translating each individual tube. A control interface that allows users to control directly the rotation, curvature, and translation of each controllable section could be easily developed for this system.

Regarding the 3D tracking system, the uncalibrated stereo cameras can be replaced with a binocular stereo vision system. The 3D reconstruction algorithm can be refined in two aspects separately: segmentation and stereo matching. An machine-learning-based segmentation strategy will be more robust for 3D tracking of the system in dynamic environments, where color and lightning continue to change (for example, during surgical operation) [30]. In stereo matching, as we are mostly interested in the axis of the entire CTR, it might be a good strategy to perform a spline interpolation on each of the segmented images before matching them. This makes sure the 2D representation of each CTR on each image is a 1D shape. More than that, performing stereo matching and 3D reconstruction on the interpolated lines would be easier as the order of each point on the CTR (from the origins to the tips of the CTR) is known.

The system will need a lot more improvement and validation before being able to be used for healthcare applications. However, due to its small size and flexibility, it will be a valuable tool for minimally invasive surgery and will help reduce the damage caused by the traditional method [31].

5 EQUALITY, DIVERSITY & INCLUSION

Although the eyeball shapes do not differ between different ethnics [32], the cranial shapes might differ [33]. As the system targets a universal population, future work in the project should validate the system in

different anatomical variations. One advantage of our system is that, if one's anatomy differs so much from the general population – whether physiological or pathological – the shape-changing ability of nitinol allows the same system to adapt to each personal characteristic.

6 CONCLUSION

The project proposes a novel compact modular design for achieving two independently controllable curved sections. The modular approach allows the same design to be used for building systems with three or more controllable curved sections theoretically. The manufacturing strategy mentioned offers a fast and economical protocol for creating balanced pairs. Although the algorithm for 3D tracking of the entire CTR requires more improvement for practical use, it is a novel approach and can be used as a foundation for further work in the future. Future research might try different laser-machined patterns and should reuse the old materials whenever possible to reduce the environmental risk. However, the benefits of a good system in a surgical context will finally outweigh the costs in the development process. A systematic evaluation of the system's stability is essential to mitigate health risks during surgical use. Further work on this system includes completing and validating the machine on eyeball and skull models, building an intuitive control interface, changing the cameras to a binocular stereo vision system, and improving in the segmentation and stereo matching algorithms of the 3D track system.

7 REFERENCES

[1] O. Adesina and B. C. Patel, "Optic Nerve Decompression," in *StatPearls*, Treasure Island (FL): StatPearls Publishing, 2024. Accessed: Aug. 20, 2024. [Online]. Available: http://www.ncbi.nlm.nih.gov/books/NBK538300/

[2] P. E. Dupont, J. Lock, B. Itkowitz, and E. Butler, "Design and Control of Concentric-Tube Robots," *IEEE Trans. Robot. Publ. IEEE Robot. Autom. Soc.*, vol. 26, no. 2, pp. 209–225, Apr. 2010, doi: 10.1109/TRO.2009.2035740.

[3] Z. Mitros *et al.*, "Optic Nerve Sheath Fenestration With a Multi-Arm Continuum Robot," *IEEE Robot. Autom. Lett.*, vol. 5, no. 3, pp. 4874–4881, Jul. 2020, doi: 10.1109/LRA.2020.3005129.

[4] Y.-C. Wu, H.-Y. Ma, Z.-H. Kuo, M. Teng, and C.-Y. Lin, "Electromagnetic Tracking System Design for Location and Orientation Estimation," in *2022 IEEE/ASME International Conference on Advanced Intelligent Mechatronics (AIM)*, Jul. 2022, pp. 1256–1262. doi: 10.1109/AIM52237.2022.9863273.

[5] A. Islam, M. Asikuzzaman, M. O. Khyam, M. Noor-A-Rahim, and M. R. Pickering, "Stereo Vision-Based 3D Positioning and Tracking," *IEEE Access*, vol. 8, pp. 138771–138787, 2020, doi: 10.1109/ACCESS.2020.3011360.

[6] OpenAI, *GPT-4o [Large language model]*. (2024). [Online]. Available: https://chat.openai.com/

[7] Anthropic, *Claude 3 [Large language model]*. (2024). [Online]. Available: https://www.anthropic.com/

[8] T. K. Morimoto and A. M. Okamura, "Design of 3-D Printed Concentric Tube Robots," *IEEE Trans. Robot. Publ. IEEE Robot. Autom. Soc.*, vol. 32, no. 6, pp. 1419–1430, Dec. 2016, doi:

10.1109/TRO.2016.2602368.

[9] C. Rucker, J. Childs, P. Molaei, and H. B. Gilbert, “Transverse Anisotropy Stabilizes Concentric Tube Robots,” *IEEE Robot. Autom. Lett.*, vol. 7, no. 2, pp. 2407–2414, Apr. 2022, doi: 10.1109/LRA.2022.3140441.

[10] D.-Y. Lee *et al.*, “Anisotropic Patterning to Reduce Instability of Concentric-Tube Robots,” *IEEE Trans. Robot.*, vol. 31, no. 6, pp. 1311–1323, Dec. 2015, doi: 10.1109/TRO.2015.2481283.

[11] K. A. X. J. Luo, J. Kim, T. Looi, and J. Drake, “Design Optimization for the Stability of Concentric Tube Robots,” *IEEE Robot. Autom. Lett.*, vol. 6, no. 4, pp. 8309–8316, Oct. 2021, doi: 10.1109/LRA.2021.3102306.

[12] D. Zhang, J. Wang, X. Yang, S. Song, and M. Q.-H. Meng, “RRT*-smooth Algorithm Applied to Motion Planning of Concentric Tube Robots,” in *2018 IEEE International Conference on Information and Automation (ICIA)*, Aug. 2018, pp. 487–493. doi: 10.1109/ICInfA.2018.8812514.

[13] Y. Lu, C. Zhang, S. Song, and M. Q.-H. Meng, “Precise motion control of concentric-tube robot based on visual servoing,” in *2017 IEEE International Conference on Information and Automation (ICIA)*, Jul. 2017, pp. 299–304. doi: 10.1109/ICInfA.2017.8078923.

[14] K. Wu, L. Wu, and H. Ren, “An image based targeting method to guide a tentacle-like curvilinear concentric tube robot,” in *2014 IEEE International Conference on Robotics and Biomimetics (ROBIO 2014)*, Dec. 2014, pp. 386–391. doi: 10.1109/ROBIO.2014.7090361.

[15] D. C. Rucker, B. A. Jones, and R. J. Webster III, “A Geometrically Exact Model for Externally Loaded Concentric-Tube Continuum Robots,” *IEEE Trans. Robot.*, vol. 26, no. 5, pp. 769–780, Oct. 2010, doi: 10.1109/TRO.2010.2062570.

[16] R. Xu, A. Asadian, S. F. Atashzar, and R. V. Patel, “Real-time trajectory tracking for externally loaded concentric-tube robots,” in *2014 IEEE International Conference on Robotics and Automation (ICRA)*, May 2014, pp. 4374–4379. doi: 10.1109/ICRA.2014.6907496.

[17] R. Xu, A. Asadian, A. S. Naidu, and R. V. Patel, “Position control of concentric-tube continuum robots using a modified Jacobian-based approach,” in *2013 IEEE International Conference on Robotics and Automation*, May 2013, pp. 5813–5818. doi: 10.1109/ICRA.2013.6631413.

[18] Z. Mitros, M. Khadem, C. Seneci, S. Ourselin, L. Da Cruz, and C. Bergeles, “Towards Modelling Multi-Arm Robots: Eccentric Arrangement of Concentric Tubes,” in *2018 7th IEEE International Conference on Biomedical Robotics and Biomechatronics (Biorob)*, Aug. 2018, pp. 43–48. doi: 10.1109/BIOROB.2018.8488091.

[19] “OpenCV: Camera Calibration and 3D Reconstruction.” Accessed: Aug. 21, 2024. [Online]. Available: https://docs.opencv.org/4.x/d9/d0c/group__calib3d.html

[20] S. Macenski, T. Foote, B. Gerkey, C. Lalancette, and W. Woodall, “Robot Operating System 2: Design, architecture, and uses in the wild,” *Sci. Robot.*, vol. 7, no. 66, p. eabm6074, May 2022, doi: 10.1126/scirobotics.abm6074.

[21] H. Kam, S.-H. Lee, T. Park, and C.-H. Kim, “RViz: a toolkit for real domain data visualization,” *Telecommun. Syst.*, vol. 60, pp. 1–9, Oct. 2015, doi: 10.1007/s11235-015-0034-5.

[22] O. Business a PTC, “Onshape | Product Development Platform.” Accessed: Aug. 21, 2024. [Online]. Available: https://www.onshape.com/en/

[23] M. Borovinšek, J. Williams, T. Svilans, and J. Michalski, *PrePoMax*. [Online]. Available: https://prepomax.fs.um.si/contributions/

[24] D. Guido and K. Wittig, *CalculiX*. [Online]. Available: https://www.dhondt.de/

[25] OpenCV, “Open Source Computer Vision Library.” 2015.

[26] Y.-M. Song, S. Noh, J. Yu, C. Park, and B. Lee, *Background subtraction based on Gaussian mixture models using color and depth information*. 2015, p. 135. doi: 10.1109/ICCAIS.2014.7020544.

[27] M. U. Farooq, W. Y. Kim, and S. Y. Ko, “A cost-effective and miniaturized actuation system for two three-tube concentric tube robots with parallel actuation,” in *2017 17th International Conference on Control, Automation and Systems (ICCAS)*, Oct. 2017, pp. 1382–1386. doi: 10.23919/ICCAS.2017.8204208.

[28] P. Anibaldi *et al.*, “Effect of Vaporized Hydrogen Peroxide and Nitrogen Dioxide Sterilization on Nitinol,” *Biomed. Instrum. Technol.*, vol. 58, no. 1, pp. 1–6, Jan. 2024, doi: 10.2345/0899-8205-58.1.1.

[29] Z. Zimiao, Z. Hao, X. Kai, W. Yanan, and Z. Fumin, “A non-iterative calibration method for the extrinsic parameters of binocular stereo vision considering the line constraints,” *Measurement*, vol. 205, p. 112151, Dec. 2022, doi: 10.1016/j.measurement.2022.112151.

[30] S. Minaee, Y. Boykov, F. Porikli, A. Plaza, N. Kehtarnavaz, and D. Terzopoulos, “Image Segmentation Using Deep Learning: A Survey,” Nov. 14, 2020, *arXiv*: arXiv:2001.05566. doi: 10.48550/arXiv.2001.05566.

[31] A. St. John, I. Caturegli, N. S. Kubicki, and S. M. Kavic, “The Rise of Minimally Invasive Surgery: 16 Year Analysis of the Progressive Replacement of Open Surgery with Laparoscopy,” *JSLS J. Soc. Laparosc. Robot. Surg.*, vol. 24, no. 4, p. e2020.00076, 2020, doi: 10.4293/JSLS.2020.00076.

[32] I. Bekerman, P. Gottlieb, and M. Vaiman, “Variations in Eyeball Diameters of the Healthy Adults,” *J. Ophthalmol.*, vol. 2014, p. 503645, 2014, doi: 10.1155/2014/503645.

[33] T. E. Bakken, A. M. Dale, and N. J. Schork, “A Geographic Cline of Skull and Brain Morphology among Individuals of European Ancestry,” *Hum. Hered.*, vol. 72, no. 1, pp. 35–44, Sep. 2011, doi: 10.1159/000330168.